

Supporting Material

Intra- and Intersubunit Dynamic Binding in Kv4.2 Channel Closed-State Inactivation

Jessica Wollberg¹ and Robert Bähring^{1,*}

¹Institut für Zelluläre und Integrative Physiologie, Zentrum für Experimentelle Medizin,
Universitätsklinikum Hamburg-Eppendorf, Hamburg, Germany

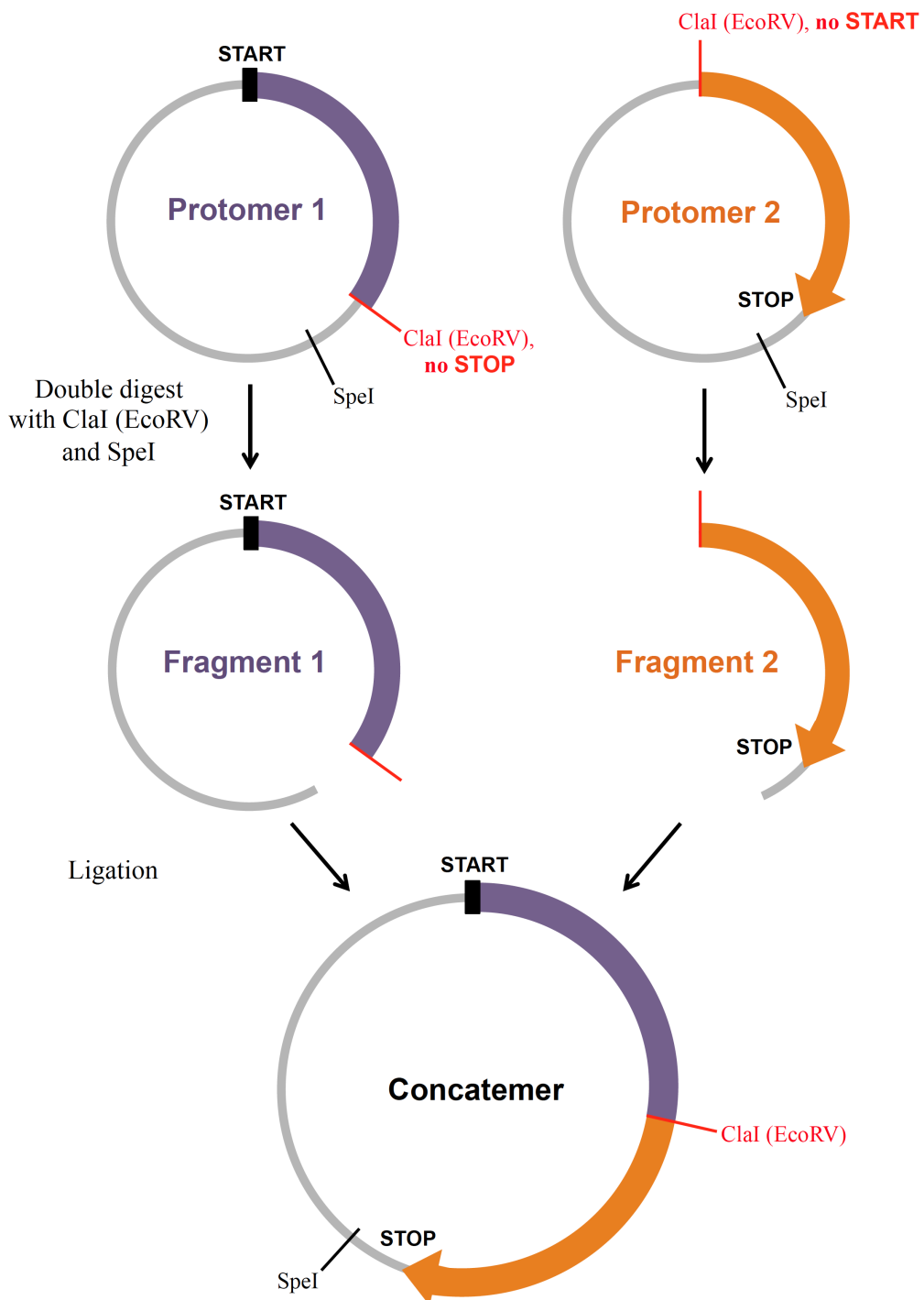


FIGURE S1 Cloning strategy for the generation of concatenated Kv4.2 tandem-dimer cDNA. Protomer 1: Endogenous *SpeI* site and engineered unique six-bases restriction site for *ClaI* (or *EcoRV*) instead of a stop codon (red); Kv4.2 coding sequence 1 in purple. Protomer 2: Endogenous *SpeI* site and engineered unique six-bases restriction site for *ClaI* (or *EcoRV*) instead of a start codon (red); Kv4.2 coding sequence 2 in orange. Double digest with *ClaI* (or *EcoRV*) and *SpeI* yields two different fragments: Fragment 1: START - Kv4.2 - *ClaI* (EcoRV); Fragment 2: *ClaI* (EcoRV) - Kv4.2 - STOP. Ligation (Fragment 2 into Fragment 1) results in concatenated cDNA (Concatemer). Point mutations were introduced before concatenation (i.e., in the protomers).

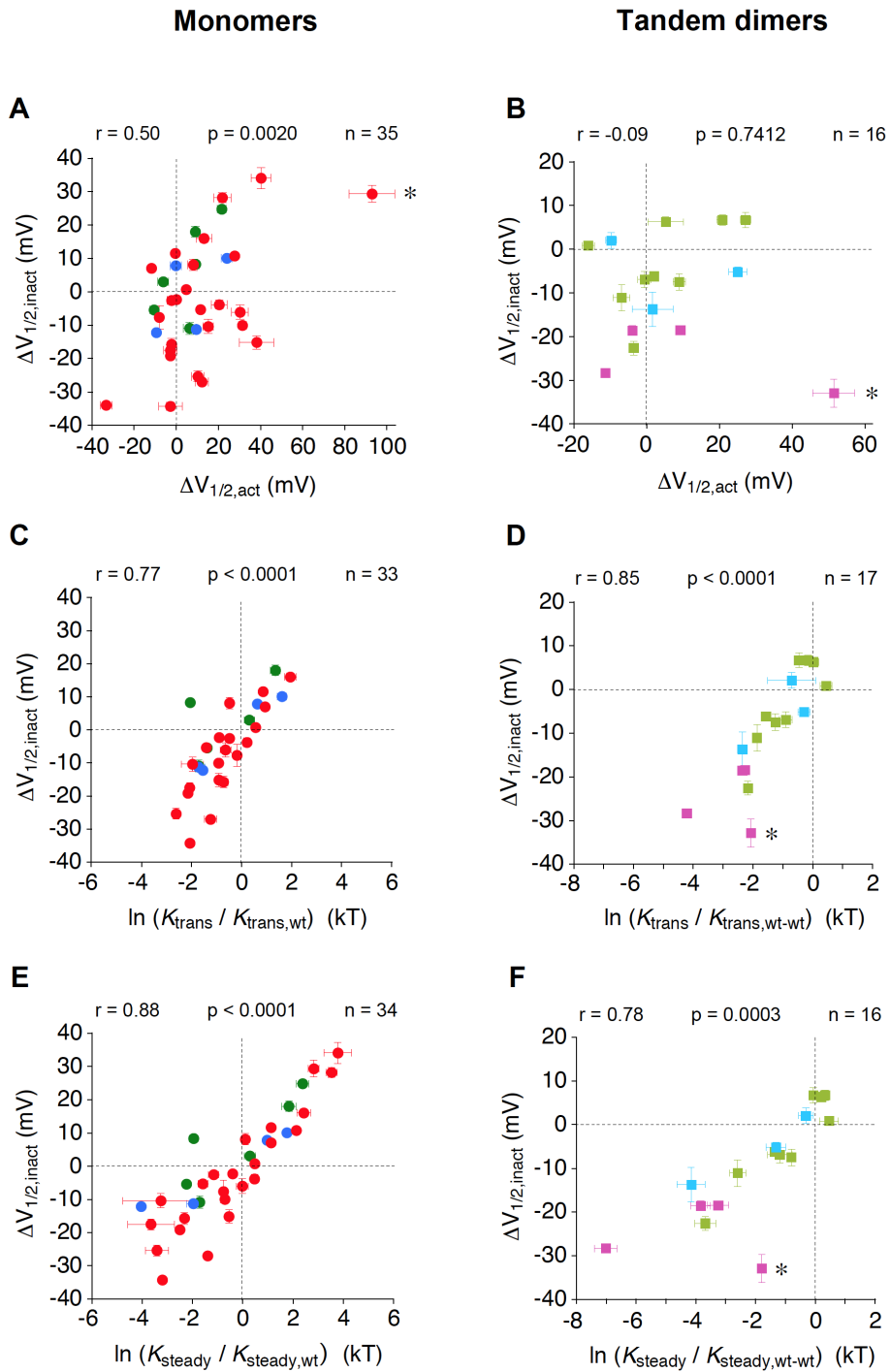


FIGURE S2 Correlation analyses for effects on low-voltage inactivation and effects on the voltage dependences of activation and inactivation for Kv4.2 mutants. Left: monomers (green: S4S5 single mutants, blue: S6 single mutants, red: double mutants); right: tandem dimers (light green: single mutants, light blue: double mutants intra-subunit configuration, magenta: double mutants inter-subunit configuration). For each construct the mutation-induced shift in the voltage dependence of isochronal (30 s prepulse) inactivation ($\Delta V_{1/2,\text{inact}}$) is plotted against the corresponding shift in the voltage dependence of peak conductance activation ($\Delta V_{1/2,\text{act}}$; *A* and *B*), the corresponding change in affinity for the transitory state expressed as $\ln(K_{\text{trans}}/K_{\text{trans},\text{wt}})$ (*C*) or $\ln(K_{\text{trans}}/K_{\text{trans},\text{wt-wt}})$ (*D*) and the corresponding change in affinity for steady-state inactivation expressed as $\ln(K_{\text{steady}}/K_{\text{steady},\text{wt}})$ (*E*) or $\ln(K_{\text{steady}}/K_{\text{steady},\text{wt-wt}})$ (*F*; see Table S1 for the analysis of voltage dependences, and Materials and Methods for the quantification of mutation-induced effects on low-voltage inactivation). Intersection points of dashed lines represent the wild-type monomer (left) or the wild-type dimer (in the absence or presence of auxiliary subunits, right). Two-tailed Pearson correlation analysis (r = Pearson correlation coefficient) was employed to test for an interdependence between the plotted parameters ($p < 0.05$). Significant correlations were found between the mutation-induced shift in the voltage dependence of inactivation and change in affinity for transitory and steady-state inactivation for both monomers and dimers. A significant correlation between the mutation-induced shifts in the voltage dependence of inactivation and activation was only found for the monomers. Asterisk in *A*: [311:408]; asterisks in *B*, *D* and *F*: [404]-[326] (see also Table S1).

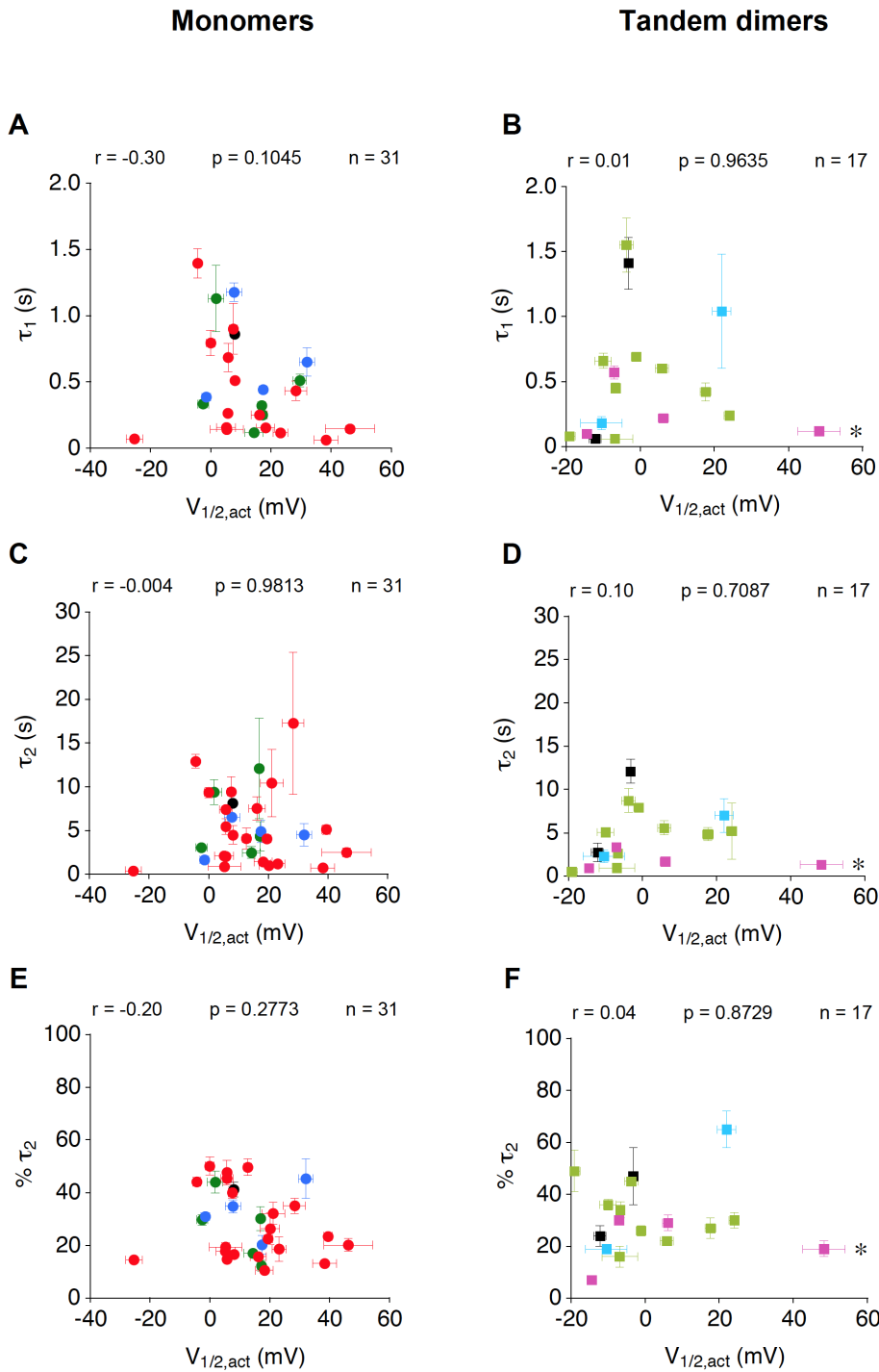


FIGURE S3 Correlation analyses of low-voltage inactivation kinetics and the voltage dependence of activation for wild-type and mutant Kv4.2 channels. Left: monomers (black: wild-type, green: S4S5 single mutants, blue: S6 single mutants, red: double mutants); right: tandem dimers (black: wild-type dimer in the absence and presence of auxiliary subunits, light green: single mutants, light blue: double mutants intra-subunit configuration, magenta: double mutants inter-subunit configuration). For each construct τ_1 (A and B), τ_2 (C and D) and the percentage of the total decay (i.e., to reach ss) accounted for by τ_2 (E and F) is plotted against the corresponding voltage for half-maximal peak conductance activation ($V_{1/2,\text{act}}$, see also Tables S1 and S2). Two-tailed Pearson correlation analysis (r = Pearson correlation coefficient) was employed to test for an interdependence of the plotted parameters ($p < 0.05$). No significant correlations were found. Asterisks in B, D and F: [404]-[326].

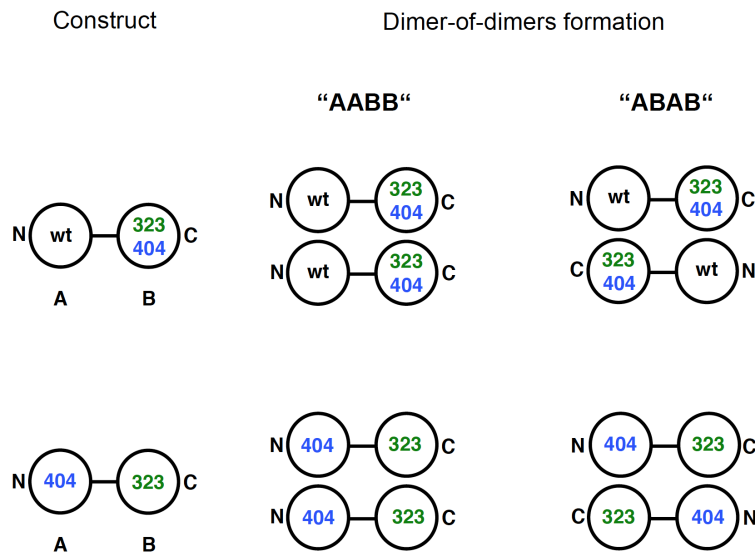


FIGURE S4 Dimer-of-dimers formation with Kv4.2 constructs. Dimer formation is schematically illustrated for the intra dimer [wt]-[323:404] and the corresponding inter dimer [404]-[323] as examples. The dimers are defined by the two entities: A (harboring the N-terminus, N) and B (harboring the C-terminus, C). Two different principal arrangements (AABB or ABAB) can be distinguished. In the "adjacent" AABB configuration the two N-termini point in the same direction. In the ABAB configuration, which reflects the rotational symmetry of voltage-gated sodium and calcium channels, the two N-termini point in opposite directions.

TABLE S1
Voltage dependence of activation and inactivation for monomeric and tandem-dimer Kv4.2 constructs

	$V_{1/2,act}$ (mV)	k_{act} (mV)	n	$V_{1/2,inact}$ (mV)	k_{inact} (mV)	n
[wt]	+8.03 ± 0.56	29.9 ± 1.21	10	-67.3 ± 0.58	5.91 ± 0.36	7
[309]	-2.47 ± 1.90	29.6 ± 0.61	5	-75.0 ± 0.61	4.90 ± 0.13	5
[311]	+17.0 ± 1.08	29.8 ± 0.33	6	-51.6 ± 1.57	7.44 ± 0.39	4
[313]	+14.4 ± 3.01	39.3 ± 3.62	5	-80.4 ± 1.82	9.66 ± 1.93	4
[322]	+1.84 ± 2.62	25.7 ± 0.94	8	-64.3 ± 1.03	6.05 ± 0.82	5
[323]	+17.3 ± 1.34	37.8 ± 1.52	7	-79.1 ± 0.62	6.76 ± 0.24	6
[326]	+29.7 ± 2.16	35.4 ± 2.43	5	-44.8 ± 0.50	6.86 ± 0.09	5
[400]	-	-		-96.3 ± 2.36	8.81 ± 0.52	3
[404]	+17.5 ± 0.68	36.3 ± 0.86	5	-78.6 ± 0.54	6.60 ± 0.33	4
[407]	+7.80 ± 2.62	28.9 ± 1.09	3	-61.8 ± 0.07	5.75 ± 0.18	3
[408]	+32.1 ± 2.49	35.8 ± 1.38	8	-57.2 ± 0.87	6.48 ± 0.67	7
[412]	-1.44 ± 1.45	29.5 ± 1.07	3	-81.7 ± 0.56	4.85 ± 0.35	3
[309:404]	+20.2 ± 3.20	54.3 ± 3.92	6	-96.6 ± 0.84	5.25 ± 0.26	6
[309:407]	+5.80 ± 2.10	31.0 ± 0.68	5	-72.1 ± 0.88	4.29 ± 0.34	5
[309:408]	+21.2 ± 3.86	30.8 ± 1.17	5	-53.5 ± 1.19	4.49 ± 0.32	5
[309:412]	+39.5 ± 1.38	50.8 ± 2.71	3	-79.6 ± 1.10	11.4 ± 0.66	4
[311:400]	+12.7 ± 1.34	38.1 ± 1.20	3	-68.9 ± 0.50	11.8 ± 0.24	3
[311:404]	+19.5 ± 1.46	36.7 ± 0.64	4	-74.9 ± 0.65	5.95 ± 0.35	4
[311:407]	+30.0 ± 4.10	29.9 ± 2.26	4	-41.4 ± 1.47	5.57 ± 0.75	4
[311:408]	+101 ± 10.9	55.6 ± 3.33	3	-40.2 ± 2.51	9.64 ± 1.13	5
[311:412]	+28.4 ± 3.67	42.6 ± 2.31	4	-71.1 ± 1.36	13.2 ± 0.60	3
[313:400]	-25.3 ± 2.72	54.4 ± 9.11	4	-104 ± 1.05	6.40 ± 0.28	4
[313:404]	-	-		-	-	
[313:407]	+16.2 ± 2.74	37.1 ± 3.97	4	-61.5 ± 1.69	8.82 ± 0.22	4
[313:408]	+38.4 ± 4.01	43.5 ± 2.27	5	-75.6 ± 2.18	10.5 ± 1.33	4
[313:412]	+5.25 ± 3.18	32.6 ± 1.15	4	-84.8 ± 1.61	10.2 ± 0.70	5
[322:400]	+5.80 ± 0.50	33.1 ± 1.04	5	-83.1 ± 1.73	6.88 ± 0.24	5
[322:404]	+18.3 ± 2.97	39.6 ± 1.38	5	-92.7 ± 1.66	7.37 ± 0.58	4
[322:407]	+7.56 ± 1.34	28.3 ± 0.40	3	-58.0 ± 0.87	8.99 ± 0.75	3
[322:408]	-	-		-55.9 ± 1.05	8.41 ± 0.47	3
[322:412]	0.002 ± 1.43	29.0 ± 1.04	6	-77.2 ± 3.42	8.72 ± 1.55	5
[323:400]	+5.32 ± 5.48	49.9 ± 6.72	4	-104 ± 1.10	6.52 ± 0.30	5
[323:404]	+23.2 ± 2.38	44.2 ± 1.54	10	-77.7 ± 2.12	6.78 ± 0.93	4
[323:407]	+8.14 ± 1.16	33.4 ± 1.67	3	-69.6 ± 0.11	6.32 ± 0.28	4
[323:408]	-	-		-74.3 ± 0.88	7.17 ± 0.56	3
[323:412]	+5.75 ± 0.68	34.4 ± 0.20	4	-88.8 ± 0.52	9.27 ± 0.26	4
[326:400]	-4.31 ± 0.55	24.2 ± 0.16	5	-62.6 ± 0.34	5.51 ± 0.23	5
[326:404]	+46.3 ± 8.20	53.0 ± 2.66	8	-84.2 ± 2.01	8.75 ± 1.05	6
[326:407]	+48.3 ± 4.63	43.0 ± 3.08	8	-35.5 ± 3.20	13.6 ± 2.07	5
[326:408]	-	-		-	-	
[326:412]	+35.8 ± 1.38	48.3 ± 2.40	5	-56.6 ± 0.98	9.24 ± 0.46	7

[wt]-[wt]	-3.13 ± 1.28	32.3 ± 0.75	3	-62.9 ± 0.60	4.72 ± 0.18	3
[wt]-[309]	-3.69 ± 1.84	23.7 ± 1.85	3	-69.8 ± 1.81	4.63 ± 0.25	3
[412]-[wt]	-6.63 ± 0.76	26.8 ± 1.26	7	-85.5 ± 1.56	7.44 ± 0.81	7
[412]-[309]	-6.98 ± 0.96	27.2 ± 1.14	5	-81.5 ± 1.09	7.10 ± 0.16	5
[wt]-[wt] (+K+D)	-12.1 ± 1.65	23.7 ± 0.51^a	4	-64.3 ± 0.24	7.16 ± 0.31	4
[322]-[wt] (+K+D)	-	-		-71.6 ± 0.68	6.11 ± 0.20	3
[404]-[wt] (+K+D)	-6.80 ± 4.81	31.8 ± 1.93^a	6	-58.1 ± 1.11	10.9 ± 0.77	5
[322:404]-[wt] (+K+D)	-10.4 ± 5.55	30.4 ± 2.24	7	-78.0 ± 3.95	5.21 ± 0.43	7
[wt]-[322]	-1.04 ± 1.29	27.5 ± 0.21	4	-69.1 ± 0.73	6.45 ± 0.19	4
[404]-[wt]	$+24.1 \pm 1.42$	42.7 ± 1.95	12	-56.2 ± 1.70	12.0 ± 0.96	4
[404]-[322]	$+6.20 \pm 1.40$	33.1 ± 0.85	8	-81.4 ± 0.97	5.12 ± 0.52	6
[wt]-[323]	-9.94 ± 2.29	25.5 ± 0.83	5	-74.0 ± 3.03	5.54 ± 0.37	3
[wt]-[404]	-19.1 ± 1.67	18.3 ± 0.57	3	-62.1 ± 0.54	4.60 ± 0.19	3
[wt]-[323:404]	-12.8 ± 1.45	21.9 ± 0.36	5	-60.9 ± 1.84	4.47 ± 0.28	4
[404]-[323]	-14.4 ± 1.12	28.9 ± 0.39	8	-91.2 ± 0.47	5.13 ± 0.11	8
[326]-[wt]	$+17.7 \pm 1.40$	34.1 ± 0.91	5	-56.2 ± 1.17	7.11 ± 0.37	6
[326:404]-[wt]	$+22.0 \pm 2.52$	31.3 ± 2.27	6	-68.1 ± 1.07	4.64 ± 0.30	6
[wt]-[326]	$+5.90 \pm 1.74$	31.0 ± 1.33	4	-70.4 ± 1.88	6.83 ± 0.54	3
[404]-[326]	$+48.3 \pm 5.78$	50.2 ± 2.92	8	-95.8 ± 3.22	10.0 ± 0.52	5

Voltages of half-maximal activation ($V_{1/2,\text{act}}$) and inactivation ($V_{1/2,\text{inact}}$) and corresponding slope-factors (k_{act} and k_{inact}) for all Kv4.2 constructs used in the present study. Analysis of voltage dependences: Peak conductance-voltage (GV) relationships were determined based on the equation $G = I_P / (V - V_{\text{rev}})$; where I_P is the peak current amplitude at the test voltage V , and V_{rev} is the potassium reversal potential (-90 mV in our experiments). GV relationships were analysed with a fourth-order Boltzmann-function of the form $G / G_{\max} = (m / (1 + \exp((V-V')/k_{\text{act}})))^4$; where G / G_{\max} is the normalized peak conductance at the test voltage V . In some cases the GV curve did not saturate within the range of test voltages studied, and the GV data were re-normalized to m (extrapolated maximum) and re-fitted by the same equation. The voltage dependence is defined by V' (6.5% of the maximal conductance) and the slope factor k_{act} , however, the $V_{1/2,\text{act}}$ values given in the table are the voltages where the above function has a value of 0.5. The voltage dependence of isochronal (30 s prepulse) inactivation was analysed with a first-order Boltzmann-function of the form $I / I_{\max} = 1 / (1 + \exp((V - V_{1/2,\text{inact}})/k_{\text{inact}}))$; where I / I_{\max} is the relative current amplitude obtained with the prepulse voltage V . $V_{1/2,\text{inact}}$ and k_{inact} are the voltage of halfmaximal inactivation and the slope factor, respectively; ^a note that auxiliary subunit co-expression (+K+D) causes a negative shift in the voltage dependence of activation for [wt]-[wt] and [404]-[wt].

TABLE S2
Kinetics of onset of low-voltage inactivation in monomeric and tandem-dimer Kv4.2 constructs

[wt]	τ_1 (s)	τ_2 (s)	% τ_2	n
[wt]	0.86 ± 0.02	8.12 ± 0.33	41 ± 3	7
[309]	0.33 ± 0.03	3.03 ± 0.14	30 ± 2	5
[311]	0.32 ± 0.03	12.1 ± 5.76	30 ± 5	4
[313]	0.12 ± 0.01	2.47 ± 0.66	17 ± 1	4
[322]	1.13 ± 0.25	9.37 ± 1.42	44 ± 4	7
[323]	0.25 ± 0.01	4.35 ± 1.69	12 ± 2	6
[326]	-	-	-	4
[400]	0.62 ± 0.14	7.61 ± 1.02	49 ± 6	3
[404]	0.44 ± 0.03	4.90 ± 1.29	20 ± 4	4
[407]	1.18 ± 0.07	6.51 ± 0.45	35 ± 3	5
[408]	0.65 ± 0.11	4.50 ± 1.27	45 ± 8	7
[412]	0.39 ± 0.02	1.66 ± 0.03	31 ± 1	5
[309:404]	0.09 ± 0.01	1.00 ± 0.19	26 ± 6	6
[309:407]	1.03 ± 0.02	7.40 ± 0.38	45 ± 2	6
[309:408]	0.47 ± 0.05	10.4 ± 3.84	32 ± 4	5
[309:412]	0.45 ± 0.02	5.12 ± 0.55	23 ± 1	5
[311:400]	0.38 ± 0.11	4.10 ± 1.18	50 ± 3	4
[311:404]	0.26 ± 0.02	4.04 ± 0.36	23 ± 0.4	5
[311:407]	-	-	-	6
[311:408]	-	-	-	5
[311:412]	0.43 ± 0.08	17.3 ± 8.12	35 ± 3	6
[313:400]	0.07 ± 0.002	0.39 ± 0.03	15 ± 1	4
[313:404]	0.26 ± 0.03	4.98 ± 1.98	27 ± 7	3
[313:407]	0.25 ± 0.01	7.53 ± 1.34	16 ± 1	6
[313:408]	0.06 ± 0.003	0.71 ± 0.06	13 ± 1	5
[313:412]	0.15 ± 0.01	2.09 ± 0.17	18 ± 1	5
[322:400]	0.68 ± 0.11	5.45 ± 0.88	48 ± 5	5
[322:404]	0.15 ± 0.02	1.41 ± 0.28	11 ± 1	4
[322:407]	0.90 ± 0.19	9.41 ± 1.75	40 ± 2	5
[322:408]	0.64 ± 0.19	14.8 ± 3.22	37 ± 12	3
[322:412]	0.79 ± 0.09	9.35 ± 0.60	50 ± 3	6
[323:400]	0.14 ± 0.004	0.85 ± 0.05	19 ± 2	6
[323:404]	0.11 ± 0.02	1.18 ± 0.31	19 ± 5	3
[323:407]	0.51 ± 0.03	4.48 ± 1.07	17 ± 1	6
[323:408]	0.43 ± 0.03	3.12 ± 0.62	16 ± 2	6
[323:412]	0.26 ± 0.003	2.02 ± 0.11	15 ± 0.3	5
[326:400]	1.40 ± 0.11	12.9 ± 0.77	44 ± 2	5
[326:404]	0.15 ± 0.03	2.49 ± 0.53	20 ± 2	6
[326:407]	-	-	-	5
[326:408]	-	-	-	5
[326:412]	-	-	-	5

[wt]-[wt]	1.41 ± 0.20	12.1 ± 1.35	47 ± 11	3
[wt]-[309]	1.55 ± 0.21	8.71 ± 1.40	45 ± 1	4
[412]-[wt]	0.45 ± 0.04	2.63 ± 0.38	34 ± 3	6
[412]-[309]	0.57 ± 0.05	3.33 ± 0.38	30 ± 1	5
[wt]-[wt] (+K+D)	0.06 ± 0.01	2.71 ± 1.05	24 ± 4	6
[322]-[wt] (+K+D)	0.67 ± 0.03	5.86 ± 0.56	24 ± 2	4
[404]-[wt] (+K+D)	0.06 ± 0.003	0.93 ± 0.50	16 ± 4	4
[322:404]-[wt] (+K+D)	0.18 ± 0.05	2.26 ± 0.73	19 ± 1	5
[wt]-[322]	0.69 ± 0.01	7.91 ± 0.36	26 ± 2	4
[404]-[wt]	0.24 ± 0.03	5.18 ± 3.22	30 ± 3	4
[404]-[322]	0.22 ± 0.02	1.66 ± 0.31	29 ± 3	5
[wt]-[323]	0.66 ± 0.06	5.07 ± 0.35	36 ± 2	4
[wt]-[404]	0.08 ± 0.01	0.48 ± 0.18	49 ± 8	4
[wt]-[323:404]	-	-	-	5
[404]-[323]	0.10 ± 0.004	0.92 ± 0.09	7 ± 1	8
[326]-[wt]	0.42 ± 0.07	4.83 ± 0.78	27 ± 4	6
[326:404]-[wt]	1.04 ± 0.44	6.98 ± 1.96	65 ± 7	4
[wt]-[326]	0.60 ± 0.03	5.56 ± 0.80	22 ± 0.3	3
[404]-[326]	0.12 ± 0.01	1.31 ± 0.17	19 ± 3	5

Time constants of low-voltage inactivation (τ_1 and τ_2) obtained by double-exponential fitting of the onset of low-voltage inactivation; % τ_2 , relative contribution of τ_2 to the total decay (i.e., to reach ss).

TABLE S3**S4S5/S6 functional coupling analysis for monomeric and tandem-dimer Kv4.2 constructs**

	$1 - a_1$	K_{trans}	Ω_{trans}	ss	K_{steady}	Ω_{steady}	n
[wt]	0.685 ± 0.008	2.19 ± 0.08		0.457 ± 0.032	0.88 ± 0.11		7
[309]	0.358 ± 0.025	0.57 ± 0.06		0.088 ± 0.009	0.10 ± 0.01		5
[311]	0.891 ± 0.017	9.09 ± 2.08		0.837 ± 0.033	6.33 ± 2.06		4
[313]	0.286 ± 0.023	0.41 ± 0.04		0.142 ± 0.018	0.17 ± 0.02		4
[322]	0.740 ± 0.042	3.31 ± 0.49		0.540 ± 0.054	1.35 ± 0.27		7
[323]	0.224 ± 0.024	0.30 ± 0.04		0.117 ± 0.016	0.13 ± 0.02		6
[326]	-	-		0.899 ± 0.020	10.5 ± 2.79		4
[400]	0.583 ± 0.068	1.56 ± 0.49		0.195 ± 0.039	0.25 ± 0.06		3
[404]	0.292 ± 0.051	0.44 ± 0.11		0.117 ± 0.026	0.14 ± 0.03		4
[407]	0.804 ± 0.010	4.16 ± 0.29		0.700 ± 0.010	2.34 ± 0.12		5
[408]	0.911 ± 0.014	12.5 ± 2.56		0.832 ± 0.016	5.31 ± 0.62		7
[412]	0.320 ± 0.014	0.47 ± 0.03		0.016 ± 0.002	0.02 ± 0.002		5
[309:404]	0.392 ± 0.058	0.77 ± 0.26	6.78 ± 2.92	0.182 ± 0.018	0.23 ± 0.03	15.2 ± 5.03	6
[309:407]	0.576 ± 0.029	1.41 ± 0.14	1.31 ± 0.22	0.228 ± 0.031	0.31 ± 0.05	1.18 ± 0.28	6
[309:408]	0.934 ± 0.013	17.5 ± 4.27	5.41 ± 1.83	0.901 ± 0.020	11.9 ± 3.68	20.2 ± 7.47	5
[309:412]	0.468 ± 0.020	0.89 ± 0.07	7.26 ± 1.08	0.306 ± 0.023	0.45 ± 0.04	250 ± 59.4	5
[311:400]	0.791 ± 0.024	3.97 ± 0.58	1.63 ± 0.26	0.588 ± 0.029	1.47 ± 0.20	1.22 ± 0.37	4
[311:404]	0.350 ± 0.019	0.54 ± 0.05	3.34 ± 0.10	0.161 ± 0.025	0.20 ± 0.04	4.98 ± 0.09	5
[311:407]	-	-	-	0.964 ± 0.009	34.0 ± 6.86	2.01 ± 0.81	6
[311:408]	-	-	-	0.932 ± 0.014	16.2 ± 3.10	2.37 ± 0.17	5
[311:412]	0.731 ± 0.010	2.74 ± 0.15	1.40 ± 0.34	0.584 ± 0.020	1.43 ± 0.11	12.7 ± 4.77	6
[313:400]	0.146 ± 0.010	0.17 ± 0.01	1.69 ± 0.20	0.002 ± 0.002	0.002 ± 0.002	26.8 ± 0.04	4
[313:404]	0.604 ± 0.048	1.61 ± 0.36	20.0 ± 7.00	0.459 ± 0.038	0.86 ± 0.12	33.7 ± 11.6	3
[313:407]	0.575 ± 0.034	1.43 ± 0.20	1.85 ± 0.35	0.495 ± 0.041	1.05 ± 0.17	2.36 ± 0.60	6
[313:408]	0.534 ± 0.051	1.29 ± 0.33	1.80 ± 0.19	0.465 ± 0.056	0.98 ± 0.27	1.03 ± 0.34	5
[313:412]	0.221 ± 0.026	0.29 ± 0.05	3.31 ± 0.70	0.053 ± 0.027	0.06 ± 0.03	19.6 ± 11.6	5
[322:400]	0.518 ± 0.043	1.14 ± 0.19	2.07 ± 0.19	0.080 ± 0.003	0.09 ± 0.003	4.37 ± 0.08	5
[322:404]	0.140 ± 0.018	0.16 ± 0.02	1.76 ± 0.19	0.039 ± 0.020	0.04 ± 0.02	5.37 ± 0.12	4
[322:407]	0.835 ± 0.021	5.48 ± 0.88	1.15 ± 0.20	0.728 ± 0.028	2.83 ± 0.40	1.28 ± 0.22	5
[322:408]	0.866 ± 0.044	8.55 ± 3.37	2.21 ± 0.21	0.794 ± 0.045	4.26 ± 0.94	1.92 ± 0.18	3
[322:412]	0.646 ± 0.026	1.89 ± 0.18	2.64 ± 0.50	0.292 ± 0.016	0.42 ± 0.03	16.7 ± 4.74	6
[323:400]	0.222 ± 0.018	0.29 ± 0.03	1.37 ± 0.50	0.036 ± 0.004	0.04 ± 0.01	1.00 ± 0.34	6
[323:404]	0.255 ± 0.075	0.37 ± 0.13	6.26 ± 2.88	0.090 ± 0.044	0.10 ± 0.05	5.01 ± 2.94	3
[323:407]	0.475 ± 0.015	0.91 ± 0.05	1.62 ± 0.28	0.372 ± 0.013	0.59 ± 0.03	1.66 ± 0.34	6
[323:408]	0.422 ± 0.021	0.74 ± 0.07	2.27 ± 0.12	0.311 ± 0.015	0.46 ± 0.03	1.79 ± 0.13	6
[323:412]	0.205 ± 0.006	0.26 ± 0.01	4.04 ± 0.66^a	0.068 ± 0.005	0.07 ± 0.01	29.8 ± 7.48	5
[326:400]	0.850 ± 0.005	5.69 ± 0.25	-	0.730 ± 0.013	2.75 ± 0.19	1.08 ± 0.36	5
[326:404]	0.471 ± 0.029	0.92 ± 0.11	-	0.339 ± 0.019	0.52 ± 0.05	3.12 ± 0.13	6
[326:407]	-	-	-	0.961 ± 0.017	73.0 ± 43.5	2.60 ± 1.73	5
[326:408]	-	-	-	0.829 ± 0.009	4.92 ± 0.31	12.9 ± 0.02	5
[326:412]	-	-	-	0.879 ± 0.015	7.76 ± 0.99	40.2 ± 14.0^a	5

Wollberg & Bähring, Supporting Material

[wt]-[wt]	0.830 ± 0.030	5.34 ± 1.34	0.664 ± 0.065	2.18 ± 0.52	3		
[wt]-[309]	0.679 ± 0.045	2.30 ± 0.46	0.413 ± 0.090	0.83 ± 0.27	4		
[412]-[wt]	0.382 ± 0.032	0.64 ± 0.08	0.064 ± 0.015	0.07 ± 0.02	6		
[412]-[309]	0.339 ± 0.023	0.52 ± 0.05	1.90 ± 0.68	0.054 ± 0.016	0.06 ± 0.02	2.20 ± 1.28	5
[wt]-[wt] (+K+D)	0.735 ± 0.031	3.02 ± 0.44	0.646 ± 0.045	2.01 ± 0.29	6		
[322]-[wt] (+K+D)	0.406 ± 0.029	0.70 ± 0.08	0.223 ± 0.029	0.29 ± 0.05	4		
[404]-[wt] (+K+D)	0.752 ± 0.034	3.24 ± 0.49	0.709 ± 0.030	2.53 ± 0.30	4		
[322:404]-[wt] (+K+D)	0.226 ± 0.020	0.30 ± 0.03	2.53 ± 0.11	0.041 ± 0.013	0.04 ± 0.02	8.37 ± 0.05	5
[wt]-[322]	0.527 ± 0.029	1.14 ± 0.15	0.361 ± 0.028	0.57 ± 0.07	4		
[404]-[wt]	0.770 ± 0.016	3.42 ± 0.31	0.670 ± 0.029	2.11 ± 0.29	4		
[404]-[322]	0.358 ± 0.035	0.58 ± 0.10	1.26 ± 0.27	0.094 ± 0.032	0.11 ± 0.04	5.07 ± 0.10	5
[wt]-[323]	0.453 ± 0.039	0.86 ± 0.13	0.149 ± 0.033	0.18 ± 0.04	4		
[wt]-[404]	0.889 ± 0.021	8.84 ± 1.62	0.762 ± 0.058	3.96 ± 1.08	4		
[wt]-[323:404]	-	-	-	0.607 ± 0.058	1.80 ± 0.43	5.48 ± 2.68	5
[404]-[323]	0.076 ± 0.009	0.08 ± 0.01	6.62 ± 0.05	0.004 ± 0.003	0.01 ± 0.003	39.4 ± 0.02	8
[326]-[wt]	0.817 ± 0.016	4.66 ± 0.49	0.751 ± 0.013	3.07 ± 0.22	6		
[326:404]-[wt]	0.794 ± 0.039	4.23 ± 0.80	1.42 ± 0.49	0.382 ± 0.071	0.68 ± 0.18	4.40 ± 0.09	4
[wt]-[326]	0.606 ± 0.026	1.56 ± 0.17	0.496 ± 0.032	1.00 ± 0.13	3		
[404]-[326]	0.406 ± 0.026	0.70 ± 0.07	1.44 ± 0.21^a	0.269 ± 0.013	0.37 ± 0.02	2.62 ± 0.12^a	5

Coupling coefficients for the transitory state (Ω_{trans}) and steady-state inactivation (Ω_{steady}) were obtained with double-mutant cycle analysis based on K_{trans} and K_{steady} values; $K_{\text{trans}} = (1 - a_1) / a_1$; $K_{\text{steady}} = ss / (1 - ss)$. Fractions a_1 and ss were obtained with double-exponential fitting of onset of low-voltage inactivation (see Materials and Methods). ^a SEM values based on linear and independent error propagation.